

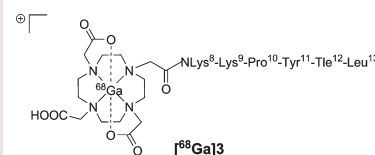
Synthesis of a ^{68}Ga -Labeled Peptoid–Peptide Hybrid for Imaging of Neurotensin Receptor Expression in Vivo

Simone Maschauer,[†] Jürgen Einsiedel,[‡] Carsten Hocke,[†] Harald Hübner,[‡] Torsten Kuwert,[†] Peter Gmeiner,[‡] and Olaf Prante^{*†}

[†]Laboratory of Molecular Imaging, Clinic of Nuclear Medicine, Friedrich-Alexander University, Schwabachanlage 6, D-91054 Erlangen, Germany and [‡]Department of Chemistry and Pharmacy, Emil Fischer Center, Friedrich-Alexander University, Schuhstrasse 19, D-91052 Erlangen, Germany

ABSTRACT The neurotensin receptor subtype 1 (NTS1) represents an attractive molecular target for imaging various tumors. Positron emission tomography (PET) gained widespread importance due to its sensitivity. We combined the design of a metabolically stable neurotensin analogue with a ^{68}Ga -radiolabeling approach. The ^{68}Ga -labeled peptoid–peptide hybrid [^{68}Ga]3 revealed high stability, specific tumor uptake (0.7% ID/g, 65 min p.i.), and advantageous biokinetics in vivo using HT29 tumor-bearing nude mice. Because of the ability to internalize into NTS1-expressing tumor cells, [^{68}Ga]3 proved to be highly suitable for a reliable and practical visualization of NTS1-expressing tumors in vivo by small animal PET.

KEYWORDS Neurotensin, neurotensin receptor, peptide, positron emission tomography (PET), gallium-68



Positron emission tomography (PET) has emerged as an imaging modality with superior sensitivity. It has been used to study the expression and activity of a variety of molecular targets such as receptors in vivo.¹ Bioactive peptides that specifically recognize their corresponding receptors in vivo represent a class of PET tracers with growing importance for imaging therapy response in the clinical surrounding.² To date, the majority of peptide-based radiopharmaceuticals are labeled with single photon emitters, such as technetium-99 m, indium-111, or iodine-123. Prominent examples are a $^{99\text{m}}\text{Tc}$ -labeled bombesin derivative ($^{99\text{m}}\text{Tc}$ [Leu13-BN), [^{111}In]octreotide (OctreoScan), or ^{125}I -labeled vasoactive intestinal peptide (^{125}I]VIP).² Recent progress has also been achieved with regard to labeling peptides with the positron emitter ^{18}F ($t_{1/2} = 110$ min).^{2,3} These approaches include rapid, chemoselective ligation methods with ^{18}F -labeled prosthetic groups.⁴ One major obstacle to developing and using PET tracers of peptide receptors is the limited availability of the radionuclides suitable for PET imaging. One solution to this problem is offered by the $^{68}\text{Ge}/^{68}\text{Ga}$ generator,^{5,6} providing frequent and easy access to the short-lived ^{68}Ga isotope ($t_{1/2} = 68$ min) multiple times a day within the generator's lifetime of about 1 year. Therefore, the $^{68}\text{Ge}/^{68}\text{Ga}$ generator system provides increased availability of the short-lived ^{68}Ga and significant cost reduction in comparison with cyclotron-produced positron emitters, such as ^{18}F . The chemistry of ^{68}Ga relies on the use of chelators that provide advantages, such as the use of very low amounts of chelator-linked peptides in aqueous buffer solution for quantitative radiolabeling reactions. However,

very few radiolabeled peptides suitable for PET imaging studies have been developed so far.² Thus, the majority of peptide receptors that are potential molecular targets for imaging of, for example, tumor response or tumor progression, have not yet been addressed by adequate peptide-based PET imaging probes.

The pivotal role of neurotensin (NT) and its receptors (NTS1, NTS2, and NTS3) in oncogenesis relies on autocrine, paracrine, and endocrine mechanisms. The crucial importance of the NTS1 expression has been demonstrated for various types of human tumors, such as breast cancer, prostate cancer, and colorectal tumors.⁷ The NT carboxy terminus NT(8–13) represents the truncated binding sequence of the natural agonist NT; however, the versatility of NTS1 imaging agents derived from NT(8–13) is frequently hampered by the low resistance of NT(8–13) toward degradation by endogenous peptidases. A variety of studies addressed this issue by modifying the amino acid sequence of NT(8–13).⁷ Among these, radiolabeled peptide candidates for therapy and in vivo imaging applications by single photon emitter tomography (SPECT) have been developed.^{8–15} However, PET offers significant advantages over SPECT, such as improved spatial resolution and sensitivity combined with the option to quantify tracer concentration in absolute units in vivo.¹⁶

Received Date: April 13, 2010

Accepted Date: May 14, 2010

Published on Web Date: May 21, 2010

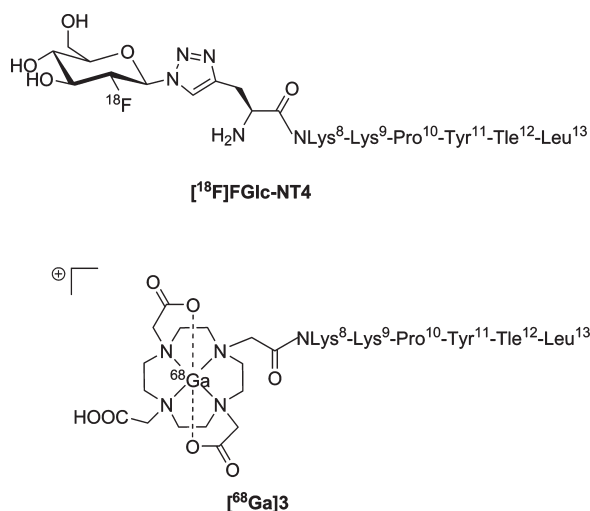


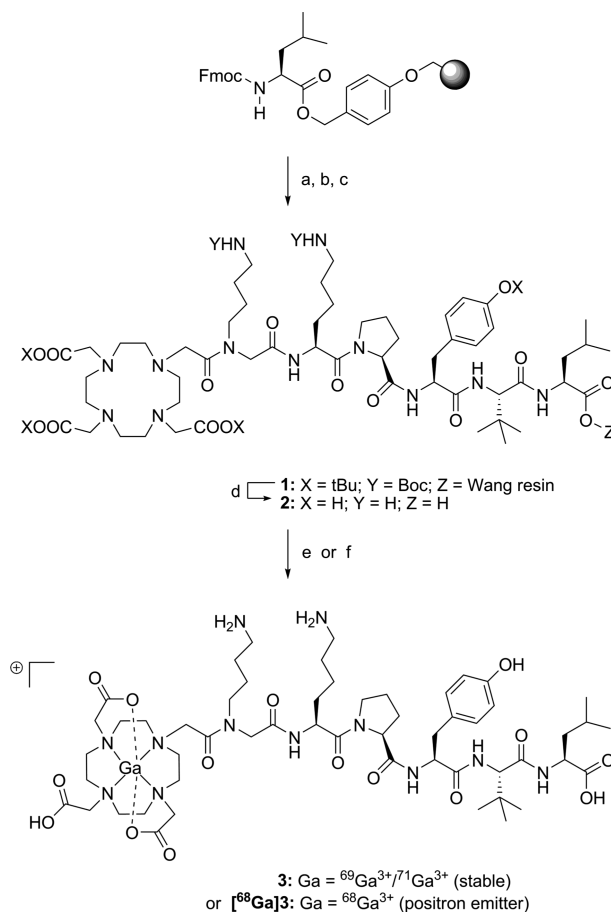
Figure 1. Chemical structure of the glycopeptoid [¹⁸F]FGlc-NT4¹⁹ and the DOTA-conjugated derivative [⁶⁸Ga]3.

On the basis of our studies on the influence of peptide backbone modifications and ligand conformation on affinity changes for a series of NT(8–13) analogues,^{17,18} we recently discovered a metabolically stabilized amino acid sequence by alteration of three amino acids in the sequence of NT(8–13), most importantly including the replacement of the *N*-terminal Arg-Arg by the peptoid-like residue *N*-(4-aminobutyl)Gly-Lys (NLys-Lys).^{17,19} These studies led to the characterization of the first metabolically stable ¹⁸F-labeled NTS1 imaging probe for PET ([¹⁸F]FGlc-NT4; see Figure 1) when we applied the strategy of an efficient click chemistry-based ¹⁸F-labeling and glycosylation method²⁰ to a NT(8–13) related amino acid sequence. The ¹⁸F-glycopeptide mimetic [¹⁸F]-FGlc-NT4 displayed a *K_i* value of 16 nM for hNTS1 and was successfully applied to small-animal PET (μ PET) studies for imaging hNTS1 expression in vivo.¹⁹ However, [¹⁸F]FGlc-NT4 showed high kidney uptake in vivo and suffered from insufficient clearance properties. Because elongation of the *N*-terminal ending of NT(8–13) is generally well-tolerated with respect to NTS recognition, we aimed at the synthesis of an *N*-terminal chelator-linked peptoid–peptide hybrid, which could provide both the opportunity for simple ⁶⁸Ga-radiolabeling by the formation of stable complexes with ⁶⁸Ga and improved biokinetic properties of the resulting ⁶⁸Ga-labeled peptide mimetic [⁶⁸Ga]3 (Figure 1).

We here report the first ⁶⁸Ga-labeled NT surrogate suitable for imaging of NT receptor expression in vivo by PET. After demonstration of binding affinity to hNTS1, radiolabeling with ⁶⁸Ga, and investigation of metabolic stability in vitro, [⁶⁸Ga]3 was successfully applied to biodistribution and μ PET studies using a HT29 xenograft nude mice model.

Our plan of synthesis was based on our previous publications on metabolically stabilized NT(8–13) derivatives (Scheme 1).^{17,19} In detail, we applied solid-phase methods with repetitive cycles of Fmoc deprotection with piperidine and acylation with the Fmoc-protected amino acids in the presence of PyBOP/HOBt, thus allowing us to incorporate *t*-leucine, proline, lysine, and *N*-(4-aminobutyl)-glycine.

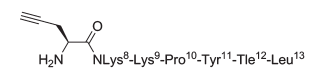
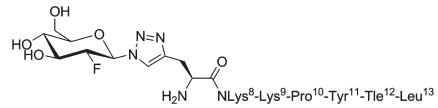
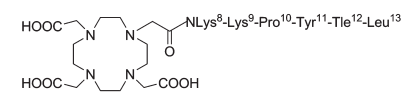
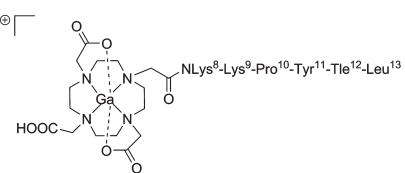
Scheme 1^a



^a Reagents and conditions: (a) (1) Piperidine/DMF (1:4), μ ~: 5 \times 5s, 100 W, 5 \times cooling to -10 $^{\circ}$ C; (2) Fmoc-*t*Leu-OH, PyBOP, DIPEA, HOBt, DMF, μ ~: 15 \times 10s, 50 W, 15 \times cooling to -10 $^{\circ}$ C. (b) (1) Fmoc deprotection (see a); (2) Fmoc-Tyr(*Or*Bu)-OH, HATU, DIPEA, DMF, μ ~-assisted coupling (see a). (c) (1) Fmoc deprotection (see a); (2) Fmoc-Pro-OH (for coupling conditions, see a), successively repeated with Fmoc-Lys(Boc)-OH, *N*-Fmoc-*N*-(4-Boc-aminobutyl)-Gly-OH, DOTA-*tr*-*t*-Bu-ester. (d) (1) H₂SO₄/dioxan (1:9), 8 $^{\circ}$ C, 2 h; (2) 30% v/v DIPEA in CH₂Cl₂; (3) TFA, phenol, H₂O, triisopropylsilane 88:5:5:2, 2 h, followed by RP-HPLC. (e) 1.2 equiv of Ga(NO₃)₃ \times H₂O, sodium acetate buffer, pH 4.5, 90 $^{\circ}$ C, 15 min, followed by the addition of 0.2 equiv of Ga(NO₃)₃ \times H₂O, 90 $^{\circ}$ C, 3 min, followed by RP-HPLC. (f) [⁶⁸Ga]GaCl₃ (200 MBq, 400 μ L), 2 (20 nmol), acetate buffer, pH 4.5, 95 $^{\circ}$ C, 10 min, > 98% (RCY).

The peptide coupling of Fmoc-Tyr(*t*Bu)-OH to the sterically demanding *t*-leucyl residue was achieved by activation with HATU. The attachment of the chelator 1,4,7,10-tetraazacyclododecane-1,4,7,10-tetraacetic acid (DOTA) was performed employing the commercially available tri-*t*-butyl ester derivative. Microwave acceleration proved to be advantageous for both Fmoc deprotection of the resin and acylation to afford **1** (Scheme 1). The direct cleavage of the peptide from the resin with TFA resulted in the formation of hardly separable *t*-butylated byproducts. This obstacle was overcome by following a previously reported protocol using 10% sulfuric acid in dioxan at 8 $^{\circ}$ C, which allowed us to safely remove the *t*-butyl-based protective groups while preventing liberation of the peptide from the solid support.²¹ Thereafter, TFA-mediated

Table 1. Receptor Binding Data of NT Analogues in Comparison with the Reference NT(8-13) as Determined by Displacement of [³H]NT Using hNTS1-Expressing CHO Cells^a

peptide	sequence	K _i (nM) ^b
NT(8-13)	Arg ⁸ -Arg ⁹ -Pro ¹⁰ -Tyr ¹¹ -Ile ¹² -Leu ¹³	0.23 ± 0.042 ^c
NT4		5.2 ± 0.92 ^c
FGlc-NT4		16 ± 2.8 ^c
2		2300 ± 1000 ^d
3		180 ± 47

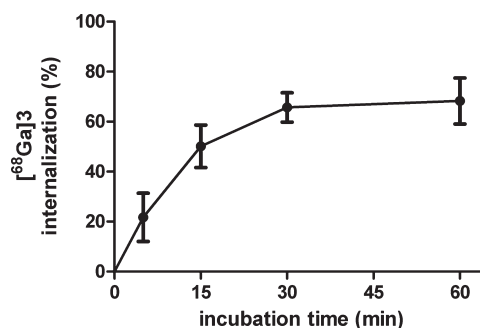
^a K_i values are based on the means of 2–7 individual experiments, each done in triplicate. ^b K_i ± SEM (nM). ^c Values are from ref 19. ^d K_i ± SD (nM).

cleavage furnished the DOTA derivative **2** sufficiently pure to allow successful high-performance liquid chromatography (HPLC) purification.

The synthesis of the Ga complex **3** was accomplished by stirring **2** with an excess of Ga(NO₃)₃ (1.4 equiv) in acetate buffer (pH 4) at 90 °C, followed by RP-HPLC purification (Scheme 1). Electrospray ionization–mass spectrometry revealed the [M]⁺ peak of **3**, confirming previous studies on DOTA-conjugated peptides with one free deprotonated carboxylate group at physiological pH that does not participate with the pseudo-octahedral geometry of the Ga–DOTA complex.

After confirmation of the high purity of **3** (> 99%) by liquid chromatography–mass spectrometry (LC-MS), we proceeded with NT receptor binding studies using a Chinese hamster ovary (CHO) cell line, stably expressing the human NTS1 as described previously.¹⁹ The Ga–DOTA conjugate **3** turned out to be significantly less potent in comparison with NT(8–13) and the previously described fluoroglycosyl-conjugated peptide mimetic FGlc-NT4 (Table 1). Notably, the DOTA-linked precursor **2** displayed a 13-fold lower NTS1 affinity when compared with the Ga–DOTA complex **3**. Thus, small amounts of **2** within the radiolabeled product solution of [⁶⁸Ga]**3** could be tolerated without significantly suppressing the specific binding of [⁶⁸Ga]**3** in vivo. The K_i values of **3** and FGlc-NT4 differed by a factor of 10. This effect could be due to the sterically demanding Ga–DOTA moiety directly linked to the pharmacophoric residue 8 of the parent peptide.¹⁴ On the other hand, the ability of agonist ligands to internalize into tumor cells via NTS1 could provide sufficient tumor labeling in vivo, even for ligands with lower affinities. Thus, we continued our efforts on the development of the ⁶⁸Ga-labeled analogue.

The radiosynthesis of [⁶⁸Ga]**3** was performed by the addition of an aliquot of the [⁶⁸Ga]GaCl₃ eluate, freshly obtained from the ⁶⁸Ge/⁶⁸Ga generator, to an aqueous-buffered solution of **2**

**Figure 2.** Time dependency of internalization of [⁶⁸Ga]**3** in HT29 cells. Data are expressed as mean values ± SDs from two independent experiments, each performed in quadruplicate.

(20 nmol, acetate buffer, pH 4.5) at 95 °C (Scheme 1). The ⁶⁸Ga-labeled peptide complex [⁶⁸Ga]**3** was obtained in a radiochemical yield (RCY) and purity of > 98% (radio-HPLC) within a total synthesis time of only 16 min. Because of the low amount of the peptide precursor (**2**, 20 nmol) that was needed for the labeling reaction and the low NTS1 affinity of **2**, we could omit a time-consuming subsequent HPLC separation of **2** and [⁶⁸Ga]**3**. The use of aqueous buffer allowed an easy formulation of [⁶⁸Ga]**3** by pH adjustment of the final product solution and a sufficient radioactivity concentration for further experimental use. The specific activity of [⁶⁸Ga]**3** was about 10 GBq/μmol at the end of radiosynthesis, rendering [⁶⁸Ga]**3** suitable for PET imaging of apparently high NT receptor densities on tumors grown as subcutaneous xenografts.

After the successful radiosynthesis of [⁶⁸Ga]**3**, we turned our attention to the stability of the ⁶⁸Ga-labeled NT analogue toward degradation by peptidases present in serum. The stability of [⁶⁸Ga]**3** was investigated in human serum at 37 °C. The HPLC data indicated high metabolic stability of 96% after an incubation time of 60 min (see the Supporting Information). Moreover, the lipophilicity (logD_{7.4}) of [⁶⁸Ga]**3** was determined to be -4.35 ± 0.26 (n = 6), and internalization studies with [⁶⁸Ga]**3** were performed in vitro using HT29 cells. The HT29 cell line is a human colon cancer cell line that expresses the hNTS1 similarly to cells from normal intestinal mucosa.²² The internalization rate of the [⁶⁸Ga]**3**/NTS1 complex into HT29 cells was approximately 70% as determined by the acid wash procedure^{19,23} after incubation with the tracer for 30 min at room temperature (Figure 2). The ability of [⁶⁸Ga]**3** to internalize in vitro suggested enhanced retention of this tracer in NTS1-expressing tumors in vivo, thus prompting us to perform biodistribution studies.

We investigated the biodistribution of [⁶⁸Ga]**3** in HT29 xenografted nude mice at 10, 30, and 65 min postinjection (p.i.; Figure 3). [⁶⁸Ga]**3** demonstrated metabolic stability in vivo (90% intact tracer in blood, 10 min p.i.; see the Supporting Information), fast blood clearance, high uptake in the kidneys, and low uptake in the liver, suggesting that hepatobiliary clearance of [⁶⁸Ga]**3** did not play a role. The markedly dominating excretion kinetics of [⁶⁸Ga]**3** occurred via fast renal clearance (Figure 3a). This notion is consistent with various other studies on DOTA-conjugated peptides,^{23,24} reflecting the effect of the free carboxylate group of the DOTA

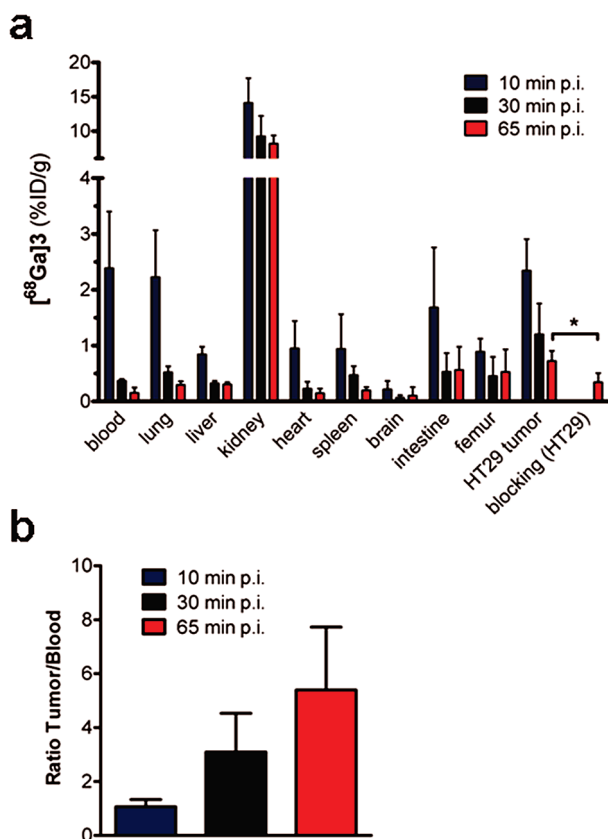


Figure 3. Biodistribution of $[^{68}\text{Ga}]\mathbf{3}$ in nude mice bearing HT29 xenografts (a) and tumor/blood ratio (b). Data are expressed as mean values \pm standard deviations (SDs) from 3 to 4 animals [$*P < 0.05$, 65 min p.i.: $0.72 \pm 0.18\%$ ID/g ($n = 3$) vs $0.34 \pm 0.17\%$ ID/g ($n = 4$)].

chelator that is unprotonated under physiological conditions. Most importantly, $[^{68}\text{Ga}]\mathbf{3}$ showed significantly lower kidney uptake and an improved kidney clearance [14.1% ID/g (10 min p.i.); 8.1% ID/g (65 min p.i.); Figure 3a] when compared to the previously described $[^{18}\text{F}]\text{FGlc-NT4}$ [data from ref 19: 57.1% ID/g (10 min p.i.); 50.0% ID/g (65 min p.i.)]. The uptake of $[^{68}\text{Ga}]\mathbf{3}$ in HT29 tumors was similar (1.2% ID/g at 30 min p.i.; 0.7% ID/g at 65 min p.i.) to our ^{18}F -labeled glycopeptide mimetic, 19 with tumor/blood ratios rapidly increasing from 1.1 to 5.4 (10–65 min p.i.; Figure 3b). This indicates a suitable signal/noise ratio for in vivo imaging applications at early time points after injection. The in vivo specificity of NTS1-mediated uptake of $[^{68}\text{Ga}]\mathbf{3}$ was proven by the analysis of tumor uptake in animals that were coinjected with $[^{68}\text{Ga}]\mathbf{3}$ and the high affinity NTS1 ligand NT4 19 (Table 1; $100\ \mu\text{g}/\text{animal}$). The coinjected animals revealed a significantly reduced tumor uptake in the biodistribution studies at 65 min p.i. ($P < 0.05$; Figure 3a).

Using a μPET scanner and HT29 tumor-bearing nude mice, we also demonstrated the specific visualization of NTS1 expression in vivo by $[^{68}\text{Ga}]\mathbf{3}$ (Figure 4). One day after administration of $[^{68}\text{Ga}]\mathbf{3}$ in a first PET scan, the experiment was repeated with the same animal coinjected with $[^{68}\text{Ga}]\mathbf{3}$ and an excess of NT4. A representative set of PET images including transaxial and coronal image projections is shown in Figure 4a, clearly indicating specific binding of $[^{68}\text{Ga}]\mathbf{3}$ in HT29 tumors grown as

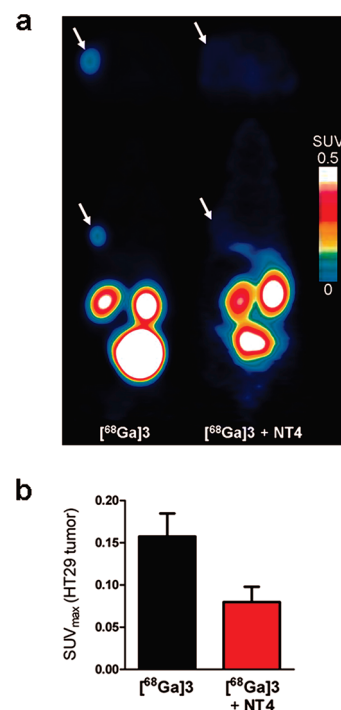


Figure 4. Static μPET images (transaxial and coronal projections) of HT29 tumor-bearing nude mice at 45–65 min postinjection of $[^{68}\text{Ga}]\mathbf{3}$ with (right) and without (left) coinjection of NT4 ($100\ \mu\text{g}/\text{mouse}$) (a) (white arrows indicate the tumor). Statistical analysis of the animal group injected with the tracer alone ($[^{68}\text{Ga}]\mathbf{3}$, $n = 3$) and the coinjected animals ($[^{68}\text{Ga}]\mathbf{3}$ + NT4, $n = 4$) (b). Maximum standard uptake values (SUV) were determined by μPET data analysis of the tumor region in each animal using the software ASI Pro. Data are expressed as mean values \pm SDs from all animals in each group.

subcutaneous xenografts, when 20 min static PET images were acquired at 45 min after injection. For each PET scan, regions of interest were drawn around the tumor and analyzed on decay-corrected whole-body coronal images. The statistical analysis of the animal group injected with the tracer alone ($n = 3$) and the coinjected animals ($n = 4$) confirmed the results obtained by the dissection analysis and revealed a significantly reduced standard uptake value (SUV) for the tumor region in coinjected animals (Figure 4b). These results provide evidence for the specificity of $[^{68}\text{Ga}]\mathbf{3}$ for imaging NTS1 expression in vivo.

In conclusion, we successfully developed $[^{68}\text{Ga}]\mathbf{3}$ as the first ^{68}Ga -labeled tracer for imaging NTS1 expression in vivo by PET. Our data confirmed that the in vitro binding affinity of a radiotracer candidate is not the only parameter that determines its suitability for in vivo imaging applications. Other factors such as the ability to internalize into cells or its lipophilicity also contribute to the in vivo binding potential of a suitable peptide radiopharmaceutical. Using $[^{68}\text{Ga}]\mathbf{3}$ as a lead compound, work is in progress toward the development of analogues with high NTS1 binding affinity to facilitate PET imaging of low receptor densities in vivo. We anticipate that $[^{68}\text{Ga}]\mathbf{3}$ and derivatives thereof have the potential to become valuable imaging agents for the exploration of NTS1 expression in various tumor types by experimental small animal PET and potentially in human PET imaging studies.

SUPPORTING INFORMATION AVAILABLE Complete experimental procedures and characterization data for compounds **1–3** and [^{68}Ga]**3**. This material is available free of charge via the Internet at <http://pubs.acs.org>.

AUTHOR INFORMATION

Corresponding Author: *To whom correspondence should be addressed. Tel: +49 9131 8544440. E-mail: olaf.prante@uk-erlangen.de.

Funding Sources: This work was supported by the Deutsche Forschungsgemeinschaft (DFG, MA 4295/1-2) and the BMBF (01EZ0808).

ACKNOWLEDGMENT We thank Bianca Weigel, I. Torres-Berger, Michaela Kettler, Michael Betz, Michael Echler, and Stefan Huber for technical assistance.

REFERENCES

- (1) Ametamey, S. M.; Honer, M.; Schubiger, P. A. Molecular imaging with PET. *Chem. Rev.* **2008**, *108*, 1501–1516.
- (2) Schottelius, M.; Wester, H. J. Molecular imaging targeting peptide receptors. *Methods* **2009**, *48*, 161–177.
- (3) Miller, P. W.; Long, N. J.; Vilar, R.; Gee, A. D. Synthesis of ^{11}C , ^{18}F , ^{15}O , and ^{13}N Radiolabels for Positron Emission Tomography. *Angew. Chem., Int. Ed. Engl.* **2008**, *47*, 8998–9035.
- (4) Wängler, C.; Schirmacher, R.; Bartenstein, P.; Wängler, B. Click-Chemistry Reactions in Radiopharmaceutical Chemistry: Fast & Easy Introduction of Radiolabels into Biomolecules for In Vivo Imaging. *Curr. Med. Chem.* **2010**, *17*, 1092–1116.
- (5) Maecke, H. R.; André, J. P. ^{68}Ga -PET Radiopharmacy: A Generator-Based Alternative to ^{18}F -Radiopharmacy. In *Ernst Schering Res Found Workshop*; Schubiger, P. A., Lehmann, L., Friebe, M., Eds.; Springer: New York, 2007; Vol. 62, pp 215–242.
- (6) Zhernosekov, K. P.; Filosofov, D. V.; Baum, R. P.; Aschoff, P.; Bihl, H.; Razbash, A. A.; Jahn, M.; Jennewein, M.; Rösch, F. Processing of generator-produced ^{68}Ga for medical application. *J. Nucl. Med.* **2007**, *48*, 1741–1748.
- (7) Myers, R. M.; Shearman, J. W.; Kitching, M. O.; Ramos-Montoya, A.; Neal, D. E.; Ley, S. V. Cancer, chemistry, and the cell: Molecules that interact with the neurotensin receptors. *ACS Chem. Biol.* **2009**, *4*, 503–525.
- (8) Buchegger, F.; Bonvin, F.; Kosinski, M.; Schaffland, A. O.; Prior, J.; Reubi, J. C.; Blauenstein, P.; Tourwé, D.; Garcia Garayoa, E.; Bischof Delaloye, A. Radiolabeled neurotensin analog, $^{99\text{m}}\text{Tc}$ -NT-XI, evaluated in ductal pancreatic adenocarcinoma patients. *J. Nucl. Med.* **2003**, *44*, 1649–1654.
- (9) de Visser, M.; Janssen, P. J.; Srinivasan, A.; Reubi, J. C.; Waser, B.; Erion, J. L.; Schmidt, M. A.; Krenning, E. P.; de Jong, M. Stabilised ^{111}In -labelled DTPA- and DOTA-conjugated neurotensin analogues for imaging and therapy of exocrine pancreatic cancer. *Eur. J. Nucl. Med. Mol. Imaging* **2003**, *30*, 1134–1139.
- (10) Garcia-Garayoa, E.; Maes, V.; Blauenstein, P.; Blanc, A.; Hohn, A.; Tourwé, D.; Schubiger, P. A. Double-stabilized neurotensin analogues as potential radiopharmaceuticals for NTR-positive tumors. *Nucl. Med. Biol.* **2006**, *33*, 495–503.
- (11) Nock, B. A.; Nikolopoulou, A.; Reubi, J. C.; Maes, V.; Conrath, P.; Tourwé, D.; Maina, T. Toward stable N4-modified neurotensins for NTS1-receptor-targeted tumor imaging with $^{99\text{m}}\text{Tc}$. *J. Med. Chem.* **2006**, *49*, 4767–4776.
- (12) Zhang, K.; An, R.; Gao, Z.; Zhang, Y.; Aruva, M. R. Radio-nuclide imaging of small-cell lung cancer (SCLC) using $^{99\text{m}}\text{Tc}$ -labeled neurotensin peptide 8–13. *Nucl. Med. Biol.* **2006**, *33*, 505–512.
- (13) Maina, T.; Nikolopoulou, A.; Stathopoulou, E.; Galanis, A. S.; Cordopatis, P.; Nock, B. A. [$^{99\text{m}}\text{Tc}$]Demotensin 5 and 6 in the NTS1-R-targeted imaging of tumours: Synthesis and preclinical results. *Eur. J. Nucl. Med. Mol. Imaging* **2007**, *34*, 1804–1814.
- (14) Alshoukr, F.; Rosant, C.; Maes, V.; Abdelhak, J.; Raguin, O.; Burg, S.; Sarda, L.; Barbet, J.; Tourwé, D.; Pelaprat, D.; Gruaz-Guyon, A. Novel Neurotensin Analogues for Radioisotope Targeting to Neurotensin Receptor-Positive Tumors. *Bioconjugate Chem.* **2009**, *20*, 1602–1610.
- (15) Garcia-Garayoa, E.; Blauenstein, P.; Blanc, A.; Maes, V.; Tourwé, D.; Schubiger, P. A. A stable neurotensin-based radiopharmaceutical for targeted imaging and therapy of neurotensin receptor-positive tumours. *Eur. J. Nucl. Med. Mol. Imaging* **2009**, *36*, 37–47.
- (16) Gambhir, S. S. Molecular imaging of cancer with positron emission tomography. *Nat. Rev. Cancer* **2002**, *2*, 683–693.
- (17) Einsiedel, J.; Hübner, H.; Hervet, M.; Härterich, S.; Koschatzky, S.; Gmeiner, P. Peptide backbone modifications on the C-terminal hexapeptide of neurotensin. *Bioorg. Med. Chem. Lett.* **2008**, *18*, 2013–2018.
- (18) Härterich, S.; Koschatzky, S.; Einsiedel, J.; Gmeiner, P. Novel insights into GPCR–peptide interactions: Mutations in extracellular loop 1, ligand backbone methylations and molecular modeling of neurotensin receptor 1. *Bioorg. Med. Chem.* **2008**, *16*, 9359–9368.
- (19) Maschauer, S.; Einsiedel, J.; Haubner, R.; Hocke, C.; Ocker, M.; Hübner, H.; Kuwert, T.; Gmeiner, P.; Prante, O. Labeling and Glycosylation of Peptides Using Click Chemistry: A General Approach to ^{18}F -Glycopeptides as Effective Imaging Probes for Positron Emission Tomography. *Angew. Chem., Int. Ed. Engl.* **2010**, *49*, 976–979.
- (20) Maschauer, S.; Prante, O. A series of 2-O-trifluoromethylsulfonyl-D-mannopyranosides as precursors for concomitant F-18-labeling and glycosylation by click chemistry. *Carbohydr. Res.* **2009**, *344*, 753–761.
- (21) Trivedi, H. S.; Anson, M.; Steel, P. G.; Worley, J. A method for selective N-Boc deprotection on Wang resin. *Synlett* **2001**, 1932–1934.
- (22) Amar, S.; Kitabgi, P.; Vincent, J. P. Activation of phosphatidylinositol turnover by neurotensin receptors in the human colonic adenocarcinoma cell line HT29. *FEBS Lett.* **1986**, *201*, 31–36.
- (23) Schottelius, M.; Berger, S.; Poethko, T.; Schwaiger, M.; Wester, H. J. Development of novel ^{68}Ga - and ^{18}F -labeled GnRH-I analogues with high GnRHR-targeting efficiency. *Bioconjugate Chem.* **2008**, *19*, 1256–1268.
- (24) Heppeler, A.; Froidevaux, S.; Mäcke, H. R.; Jermann, E.; Béhé, M.; Powell, P.; Hennig, M. Radiometal-Labelled Macrocyclic Chelator-Derivatised Somatostatin Analogue with Superb Tumour-Targeting Properties and Potential for Receptor-Mediated Internal Radiotherapy. *Chemistry* **1999**, *5*, 1974–1981.